

Design, Fabrication and Characterization of Hybrid III-V/SOI Phase-shift Free DFB Laser with Tapered Silicon waveguide

A. Gallet^{1,3}, K. Hassan², C. Jany², T. Card², J. DaFonseca², V. Rebeyrol², N. Girard¹, A. Shen¹, D. Make¹, J-G. Provost¹, J. Decobert¹, V. Muffato², A.Coquiard², S. Malhouitre², S. Olivier², H. Debrégeas¹, G.-H. Duan¹ and F. Grillot³

¹ III-V Lab, a joint lab of Nokia, Thales and CEA, Campus Polytechnique, 1, Avenue A. Fresnel, 91767 Palaiseau Cedex, France,

² CEA LETI, Minatec, 17 rue des Martyrs, F-38054 GRENOBLE cedex 9, France.

³ LTCI, Telecom ParisTech, 46 rue Barreau, 75634 Paris Cedex 13, France.

antonin.gallet@3-5lab.f

Abstract: We report on a fully integrated hybrid III-V on silicon distributed feedback laser without a phase shifter. A short intra-cavity higher index and higher grating strength section provides mode selectivity. This leads to 1.5-times more output power than standard lasers.

Introduction

Hybrid III-V on silicon-on-insulator (SOI) distributed feedback (DFB) lasers are promising sources for telecommunications, especially when used with high performance silicon modulators [1]. As it is integrated with such a component, it is easier to use $\lambda/4$ phase-shifted lasers rather than cleaving the laser and making a coating on the integrated laser facet. However, $\lambda/4$ phase shifted lasers suffer from lower external efficiencies as the power is emitted equally at both ends of the cavity. They are also much more subjected to longitudinal spatial hole burning which limits the performance of such a laser. Moreover, the precise wavelength determination of $\lambda/4$ phase-shifted laser might not be needed in coarse wavelength division multiplexing where hybrid III-V on silicon component is likely to be used. In this paper, for the first time to our knowledge, we report on a novel hybrid III-V on SOI DFB laser without phase-shift or coatings.

Operation principle and device description

The laser is fabricated by molecular bonding of the III-V material onto a SOI wafer [2] which is processed on a CMOS line using mature silicon process tools, leading to low fabrication costs. A Bragg grating is etched into the silicon waveguide. After encapsulation of the silicon and planarization of the oxide, a III-V stack is bonded and processed. The grating structure is similar to a dual-pitch laser proposed in [3] and realized in [4]. In this realisation the grating pitch Λ is kept constant but the effective refractive index is varied. Hence the two DFB sections have a Bragg wavelength $\lambda_{B1,2}$ which is slightly different. If the difference $\lambda_{B1} - \lambda_{B2}$ is equal to half the stop-band width of the first section, the

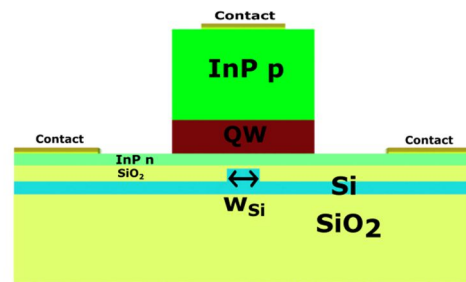


Fig. 1: Cross section of the hybrid 3-5/SOI device, showing the buried oxide, the 500-300 nm silicon rib waveguide, the 80 nm bonding oxide and the 3-5 stack.

total laser would have a preferred lasing mode. The device presented here has a long ($370 \mu\text{m}$) first section with a grating strength K_1 of 47 cm^{-1} . In the short ($30 \mu\text{m}$) second section, both grating strength K_2 and effective refractive index $n_{\text{eff},2}$ increase linearly from the values of the first section. As the refractive index in the second section is higher than in the first section, the mode with the longer wavelength is favoured. A cross section of the device is presented on fig. 1. The effective index of the hybrid mode and the confinement in the silicon waveguide increases when W_{Si} increases. The grating strength K_2 increases with W_{Si} as it is proportional to the confinement in the silicon waveguide. It means that the linear increase of n_2 and K_2 is obtained through a linear enlargement of W_{Si} . The fabrication of such a taper doesn't add any technology complexity in the CMOS process. The device structure is sketched in fig. 2a. The 500 nm thick silicon waveguide is represented in orange. The III-V stack is in red and the 300 nm thick silicon is

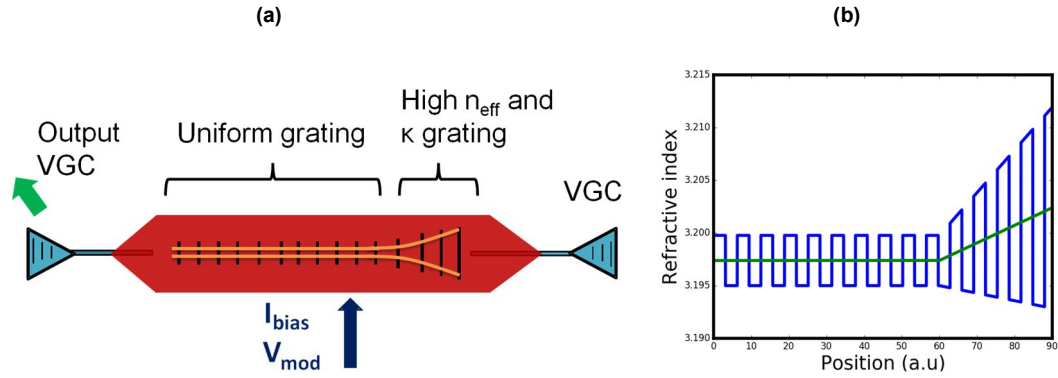


Fig. 2: (a) Two section DFB laser schematic showing the 300 nm silicon waveguide (blue), the 500 nm silicon waveguide (orange), the grating (dark), the III-V stack on top of the silicon (red). For clarity, III-V to silicon tapers are not shown. (b) Effective index variation along resonator.

blue. Light is then outcoupled by a vertical grating coupler (VGC) at the left side. The right side VGC can be used to probe the cavity power asymmetry. The mean value of K_2 is twice the value than that of the first section. The total KL product of the grating is around 2. The variation of effective index and kappa is sketched on fig. 2b. Parameters of the two sections are summarized in the following table:

	Section 1	Section 2
L (μm)	370	30
Mean K (cm^{-1})	47	100
N _{eff}	3.2	$n > 3.2$
Pitch Λ (nm)	240	240

Transfer matrix method simulations and static characteristics

To validate our assumptions, simulation based on transfer matrix method [4] is performed. Cavity modes are displayed on fig. 3a. They show the breaking of the symmetry with a preferred long wavelength mode. The calculated threshold gain difference is 2.1 cm^{-1} hence enabling single mode emission with sufficient side mode suppression ratio (SMSR) [6]. Simulations indicate that the symmetry breaking comes from the index difference

between the two sections and not from the grating strength difference. The calculated spectrum (fig. 3b) has a SMSR of 50 dB. The experimental SMSR (fig. 3c) is always better than 40 dB when the bias current is varied from 100 to 150 mA. The difference between experimental and simulated stopband widths is below 5% indicating a very good agreement between experiments and modelling. The higher grating strength K_2 in the second section makes the intensity distribution in the cavity asymmetric and localized in the front of the laser and hence increases the collected power. Fig. 4a shows the calculated intensity distribution in the cavity for the proposed device. For comparison, the intensity of a phase-shifted laser is depicted, presenting 1.8x less facet power, and more risk of spatial hole burning due to high photon density at cavity center position. Simulations indicate that the increase in facet power come from the grating strength difference between the two sections. Fig. 4b shows experimental L-I curve of the laser and of a $\lambda/4$ phase shifted laser from the same bar. If the threshold is the same one can see that the two-section laser has 1.5 more power than the conventional $\lambda/4$ phase-shifted laser. The power collected at the right side of the laser is 3 dB less than the

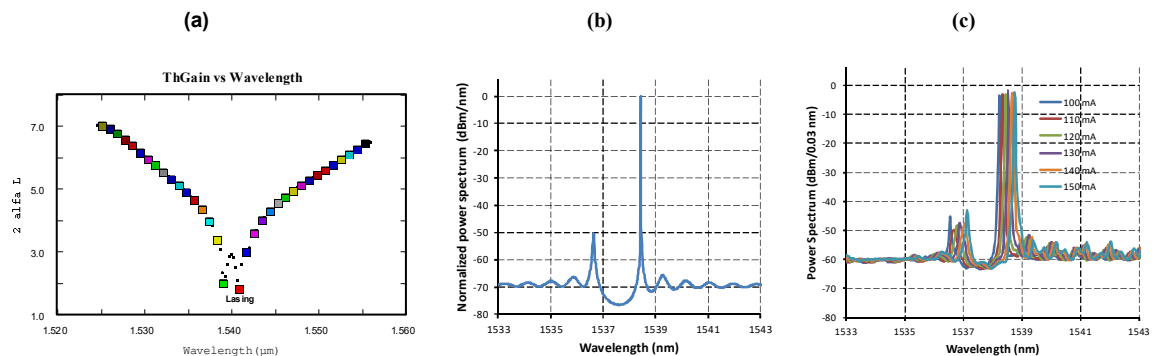


Fig. 3: (a) Threshold gain for the different modes of the hybrid DFB laser obtained by transfer matrix method. The calculation clearly indicates that lasing mode is located on the long wavelength side of the stopband. The Threshold gain difference of the structure is 2.1 cm^{-1} . (b) Calculated spectrum for $I = 2^*I_{th}$ showing SMSR of 50 dB. (c) Measured spectrum for different bias currents showing SMSR > 40 dB. The difference in stopband width is less than 5%.

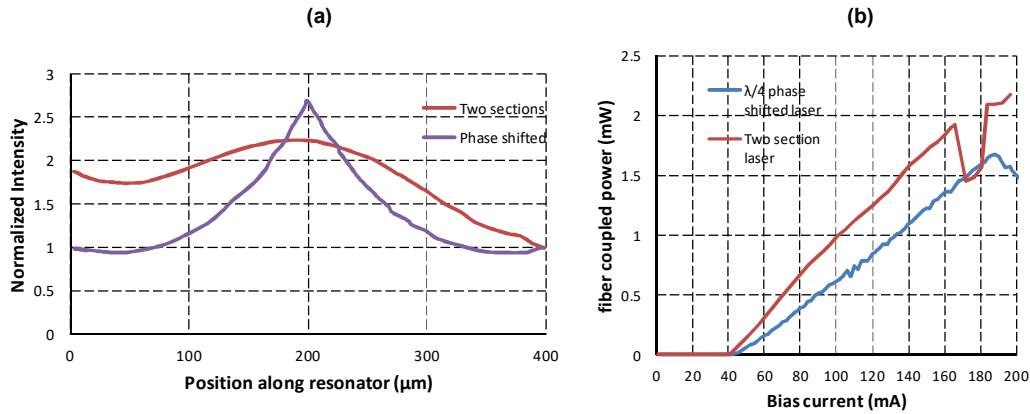


Fig. 4: (a) Normalized intensity versus position in the cavity for our device (red) and the phase shifted laser (purple). The power asymmetry between right and left side is related to the grating strength difference between the two sections. (b) L-I curve for a two section DFB laser (red) and for a standard $\lambda/4$ laser of same length and grating strength of the same bar.

power from the left side.

Direct modulation at 25 Gb/s

In order to validate the component in system conditions, direct modulation experiment is performed at 25 Gb/s. Bit error rates curves and eye diagrams are displayed on fig. 5. The laser

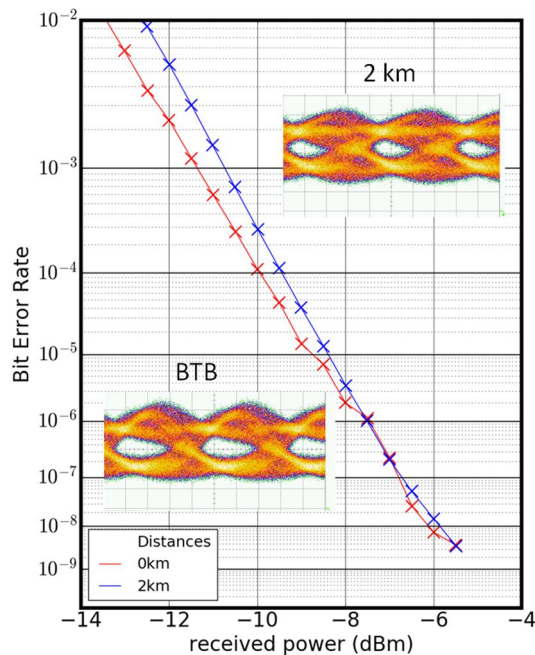


Fig. 5: Bit Error rate and eye diagram measurements at 25 Gb/s. A penalty of less than 0.5 dB is obtained after 2 km.

is biased at 140 mA and a modulated voltage is applied, resulting in 3 dB extinction ratio. The extinction ratio is limited by the maximum voltage swing available (1.7V_{pp}). The Pseudo-random-bit-sequence length is $2^{31}-1$. Error free performance is obtained for back to back and after 2 km transmission over standard single mode fiber. The penalty after 2 km is less than 0.5 dB.

Conclusion

We designed and fabricated a C-band laser with two grating sections and a stripe engineering

approach of a silicon rib waveguide. The effective index variation ensures the single mode behavior. We validated the design by using transfer matrix method based simulations. Numerical results greatly reproduce experiments and indicate that such a structure has a better efficiency than $\lambda/4$ phase shifted lasers with a gain of optical power by a factor of 1.5 thanks to an asymmetric photon emission. Direct modulation at 25 Gb/s of the laser shows error free operation after 2 km. Further work will now consider new designs to increase the cavity power asymmetry and improve bandwidth.

Acknowledgements: This work was supported in part by the European Community's Seventh Framework Program (FP7/2013-2016) under grant agreement n°619626 SEQUOIA. The authors would like to thank Richard Schatz for providing the transfer matrix software.

References

- [1] P. Doussiere, "Laser integration on silicon," *2017 IEEE 14th International Conference on Group IV Photonics (GFP)*, Berlin, 2017.
- [2] G. H. Duan et al., "New Advances on Heterogeneous Integration of III-V on Silicon", *J. Lightwave Technology*, vol. 33, no. 5, pp. 976-983, Mar. 2015
- [3] G. P. Agrawal and A. H. Bobeck, "Modeling of distributed feedback semiconductor lasers with axially-varying parameters," in *IEEE Journal of Quantum Electronics*, vol. 24, no. 12, pp. 2407-2414, Dec. 1988.
- [4] F. Grillot et al., "Analysis, fabrication, and characterization of 1.55-μm selection-free tapered stripe DFB lasers," in *IEEE Photonics Technology Letters*, vol. 14, no. 8, pp. 1040-1042, Aug. 2002
- [5] G. Bjork and O. Nilsson, "A new exact and efficient numerical matrix theory of complicated laser structures: properties of asymmetric phase-shifted DFB lasers," in *Journal of Lightwave Technology*, vol. 5, no. 1, pp. 140-146, Jan 1987
- [6] Jens Buus et al. *Tunable Laser Diodes and Related Optical Sources*, Wiley-IEEE Press, 2005,